

Using Visualization Tools to Create Kriging Models

Gary M. Stump,^{*} Jay D. Martin,[†] and Timothy W. Simpson^{1‡}
The Pennsylvania State University, University Park, PA 16802 USA

The effective use of trade space exploration requires the generation of a large number of feasible designs to permit investigation of the trade space to identify regions of interest and to understand the local tradeoffs that may exist within that region. This generation of a large number of feasible designs is often too computationally expensive to perform. The information present in a trade space can often be adequately represented with only a few points or examples, but it is difficult to interpret this information in small regions of the space with visualization tools when only a few observations are present. This work presents the use of kriging models to create surrogates to the original system analysis models and generate a large amount of surrogate designs to populate the trade space and perform trade space exploration. This work demonstrates the combination of the previously developed trade space visualization tool with new kriging model creation software. Given the graphical nature of the tool, a graphical approach to assess and update kriging approximations in regions of interest is presented. This approach allows users to leverage multi-dimensional data visualization tools to explore, understand, and identify regions of interest in the trade space. Once regions of interest have been identified, users can select points within these regions and invoke high fidelity simulation models, thereby reducing error in the surrogates.

Nomenclature

<i>Payload</i>	=	Payload supported by the space shuttle
<i>tIn</i>	=	thickness of the cylinder shell of the fuel tank
<i>R</i>	=	radius of the fuel tank

I. Introduction

Trade space exploration (TSE) is based on the Design by Shopping paradigm proposed by Balling.¹ In this alternative approach to design optimization, a large number (e.g., thousands) of designs are generated and compared on one or more criteria. From this broad collection of design alternatives, regions of interest can be identified and further investigated. TSE differs from traditional optimization because it does not require the *a priori* selection of weightings between competing performance parameters.² The Design by Shopping paradigm presents all of the design alternatives at once to the decision-maker so that a preference can be formed based upon the feasible design alternatives.³ This paradigm allows decision-makers to understand both the broad alternatives available, and, by focusing on specific regions of interest, the local behavior that exists in the design alternatives. The local behavior consists of the sensitivity to the design parameters in that region as well as the optimality of the design.⁴ Sensitivity information is important to understanding both the local tradeoffs and the robustness of the design's performance to small changes in the design parameters.

Trade space exploration, while having many advantages over traditional optimization methods, does have the disadvantage of requiring the generation of a large number of designs to fill the design trade space.³ The increasing computational capabilities available to evaluate system designs have made TSE feasible, but most designers desire to include higher fidelity models earlier in the design process to reduce the uncertainty in their predictions; however, it is frequently too computationally expensive to utilize high-fidelity modeling in TSE. One possible solution is to use surrogate models of the high-fidelity models that capture the design information present in the high-fidelity model to create virtual response surfaces, avoiding most of the large potential computational expense.⁵ The

^{*} Research Assistant, The Applied Research Laboratory, State College, PA, 16804, email: gms158@psu.edu

[†] Research Associate, The Applied Research Laboratory, State College, PA, 16804, email: jdm111@psu.edu

[‡] Professor of Mechanical and Industrial Engineering, Associate Fellow AIAA, email: tws8@psu.edu

surrogate models are best created with a combination of prior knowledge of the system being estimated to dictate the best model form and observations of the model being estimated to tune the model parameters optimally.⁶

This paper demonstrates an initial combination of visualization tools and kriging model creation tools into a single, graphically oriented application. An overview of the kriging model form and how they are created is provided in the next section. Following the kriging discussion, a review of the ATSV and visual steering work is provided. These overviews are followed by some of the details of how the two different tools were combined and the issues that were encountered during their integration. The final section shows the results of the integration and some of the initial thoughts on the future directions on this line of development..

II. Background

A. Kriging Models

A kriging model is a statistics-based model that can interpolate a set of observations.⁷ It consists of two parts. The first part, in general, quantifies long-range trends in the observations. The second part quantifies shorter range spatial correlations in the observations. The general form of a kriging model is:⁷

$$\hat{y}(\mathbf{x}) = \sum_{i=1}^k \beta_i f_i(\mathbf{x}) + Z(\mathbf{x}) \quad (1)$$

The second part, $Z(\mathbf{x})$, is a model of stationary spatial Gaussian process with zero mean and a covariance given as:

$$\text{cov}(Z(\mathbf{x}_1), Z(\mathbf{x}_2)) = \sigma^2 R(\mathbf{x}_1, \mathbf{x}_2). \quad (2)$$

The process variance, σ^2 , is a scalar parameter of the spatial correlation function (SCF), $R(\mathbf{x}_1, \mathbf{x}_2)$. The most commonly used SCF in kriging models used in engineering design is the Gaussian function.⁸ The Gaussian function offers a smooth function defined with a single parameter to control its width or range. For a d -dimensional space, the SCF is defined with a product correlation rule as:

$$R(\mathbf{x}_1, \mathbf{x}_2) = \prod_{i=1}^d e^{-\left(\frac{x_{2,i} - x_{1,i}}{\theta_i}\right)^2} \quad (4)$$

where $\mathbf{x}_{1,i}$ is the i^{th} dimension of the vector \mathbf{x}_1 and θ_i is the correlation range parameter in the i^{th} dimension. The final form of the kriging model is then given as:

$$y(\mathbf{x}) = \mathbf{f}^T(\mathbf{x})\hat{\boldsymbol{\beta}} + \mathbf{r}^T(\mathbf{x})\mathbf{R}^T(\mathbf{y} - \mathbf{F}\hat{\boldsymbol{\beta}}) \quad (5)$$

where \mathbf{R} is matrix of the estimated correlations of all of the observations, $\hat{\boldsymbol{\beta}}$ is a vector of regression coefficients, $\mathbf{f}^T(\mathbf{x})$ is a vector of the regressor functions evaluated at the current location \mathbf{x} , and \mathbf{F} is a matrix of the regressor functions evaluated as all of the observed locations. The selection of the regressors used can either be the result of statistic-based approaches that test which parameters are most likely important to the model or prior information about the system being estimated can be used to select the regressor used.

The mean square error of the kriging model estimate is given by

$$\text{MSE}[\hat{y}(\mathbf{x})] = \sigma^2 \left(1 - \mathbf{f}^T(\mathbf{x})\mathbf{r}^T(\mathbf{x}) \begin{bmatrix} \mathbf{0} & \mathbf{F}^T \\ \mathbf{F} & \mathbf{R} \end{bmatrix}^{-1} \begin{bmatrix} \mathbf{f}(\mathbf{x}) \\ \mathbf{r}(\mathbf{x}) \end{bmatrix} \right) \quad (6)$$

This estimate of the mean square error or variance of the model's estimate, $\hat{y}(\mathbf{x})$, is only valid if the residuals of the observations from the predicted trend surface have a normal or Gaussian distribution.

Given the form of the model, the next step is to estimate the best model parameters to use with that form. These parameters include the regressor coefficients $\hat{\boldsymbol{\beta}}$, and the spatial correlation ranges $\boldsymbol{\theta}$. The estimation of the process variance σ^2 is necessary only if estimates of the uncertainty in the estimated values are to be used. The most common method used to estimate the model parameters is to use the statistics-based method of Maximum Likelihood Estimation (MLE).⁷ In this method, the model parameters are chosen to maximize the likelihood of the observations. As a result, it is an optimization process. The optimal values of the trend function coefficients can be solved for in closed-form as:

$$\hat{\beta} = (\mathbf{F}^T \mathbf{R}_{\theta}^{-1} \mathbf{F})^{-1} \mathbf{F}^T \mathbf{R}_{\theta}^{-1} \mathbf{y} \quad (7)$$

where the subscript of θ on the correlation matrix, \mathbf{R} , has been included to indicate that it is still a function of spatial correlation parameters, θ . This optimal value is dependent upon being given the correlation range parameters. It is also possible to solve for the process variance as:

$$\sigma^2 = \frac{1}{n} (\mathbf{y} - \mathbf{F}\hat{\beta})^T \mathbf{R}_{\theta}^{-1} (\mathbf{y} - \mathbf{F}\hat{\beta}) \quad (8)$$

A closed-form solution does not exist for the optimal correlation range parameters. As a result, numerical optimization must be used to determine the correlation range parameters. If the optimal values for the trend function coefficients and the process variance are plugged into the likelihood equation a simplified objective function can be created. By taking the logarithm of this function, the optimization becomes

$$\begin{aligned} \text{maximize:} & \quad -\frac{n}{2} \ln[2\pi\sigma^2] - \frac{1}{2} \ln[|\mathbf{R}_{\theta}|] - \frac{n}{2} \\ \text{subject to:} & \quad \theta > 0 \end{aligned} \quad (9)$$

Even with this reduction in the dimension of the optimization problem, the optimization process can still be a computationally expensive process. The computational expense can be primarily attributed to two calculations: the evaluation of the exponential function for the elements of the correlation matrix and the inversion of the correlation matrix. In addition to the potential computational expense associated with each iteration of an optimization algorithm, there are several numerical difficulties that can arise. The three most prevalent issues are: 1) ill-conditioned correlation matrices, 2) multiple local optimum, and 3) long ridges of near optimal values.⁷ Recent work has calculated analytical gradients and Hessians for all of the model parameters for the log-likelihood function when a Gaussian spatial correlation function is used.⁹

B. Visual Steering

The Applied Research Laboratory's Trade Space Visualizer (ATSV)¹⁰ is a Java-based graphical user interface that allows users to visualize data using multidimensional data visualization techniques, as shown in Figure 1. The ATSV includes visual steering capabilities, where end users have the ability to drive underlying simulation models using commands within data visualization plots.¹¹ Examples of broad search, point-based, and Pareto search visual steering commands are illustrated in Figure 2. Visual steering provides the advantage of broadly exploring complex trade spaces, while sampling regions of interest with a higher density of points.

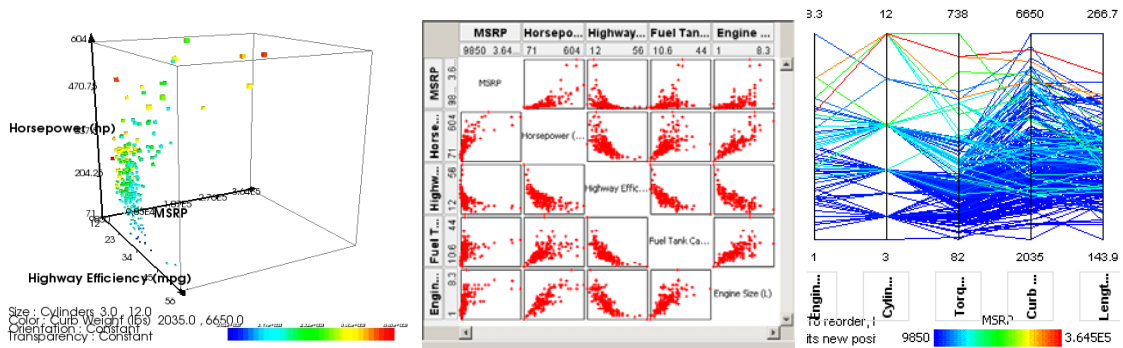


Figure 1. 3D glyph, 2D scatter matrix, and parallel coordinates plots

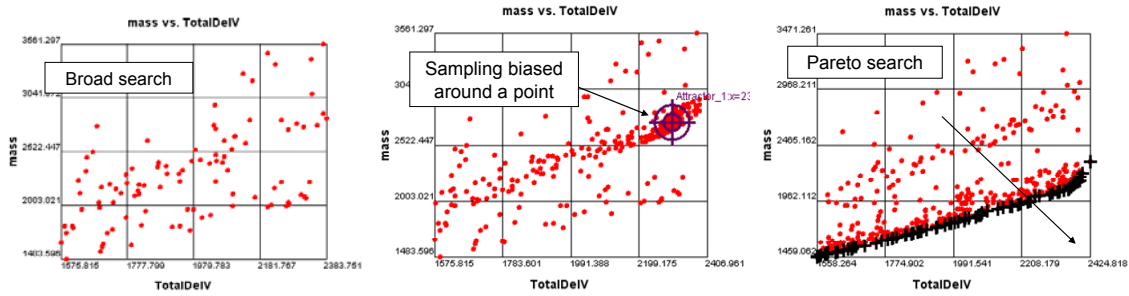


Figure 2. Examples of broad search, point-based, and Pareto search visual steering commands

Due to the need to generate large numbers of potential designs, especially when using visual steering tools, a computationally efficient system model is required. A kriging surrogate model can provide this computationally efficient model given its ability to capture highly nonlinear behavior.¹² One issue with using a kriging model to approximate the original analysis is the accuracy of the resulting surrogate. The visual tools used to explore a trade space can also be used to guide the iterative creation of an accurate surrogate model by adding additional observations in areas of most interest to the user that have high levels of uncertainty.⁶ The approach taken to perform this operation is described next.

III. Creating Kriging Models Using Visualization Tools

A. Proposed Approach

The proposed approach is a “human-in-the-loop” process, where users can visualize and refine surrogate models within regions of interest until the model’s accuracy satisfies a user-defined acceptable limit. A surrogate model is refined by displaying a response surface that represents the system performance as a function of two (or more) design parameters. The response surface is made up of a large number of pseudo-points that are created by evaluating the surrogate model at a large number of random locations in the input space. The visualization tools can also display the level of uncertainty that exists in the surrogate’s expected values through the use of color. The user can take advantage of all of the trade space exploration tools to assist them in focusing on specific regions of interest and then select a pseudo-point in which the user would like to execute the original models and use the resulting observation set to update the surrogate model.

The process used consists of five steps as shown in Figure 5. A detailed description of the iterative, human-in-the-loop process are as follows:

- Step 1** Sample the simulation model to get an initial set of feasible designs. For our initial approach, we have used Latin Hypercube sampling to fill the input space.¹³
- Step 2** Create a kriging model using the initial set of feasible designs. Our initial surrogate model approach uses kriging models, since they offer the advantage of quantifying model uncertainty at any location on the response surface;¹⁴ this uncertainty information can be used to improve accuracy within regions of interest.
- Step 3** Perform a Monte Carlo simulation on the surrogate model, where input variables are randomly varied across feasible input bounds. Input and output values for each run are captured and saved as pseudo data, which can be displayed in multidimensional data visualization plots, as shown in Figure 4.
- Step 4** Identify areas of interest and select a point to update the surrogate model. Point selection capabilities within the data visualization plots allow users to identify areas of the surrogate model that need refined.
- Step 5** Execute the simulation model at the selected point on the surrogate model. This new point is appended to the original dataset, and the surrogate model is updated with the new point. Steps 3 through 5 are repeated until the user is satisfied with the surrogate model’s accuracy within the region(s) of interest.

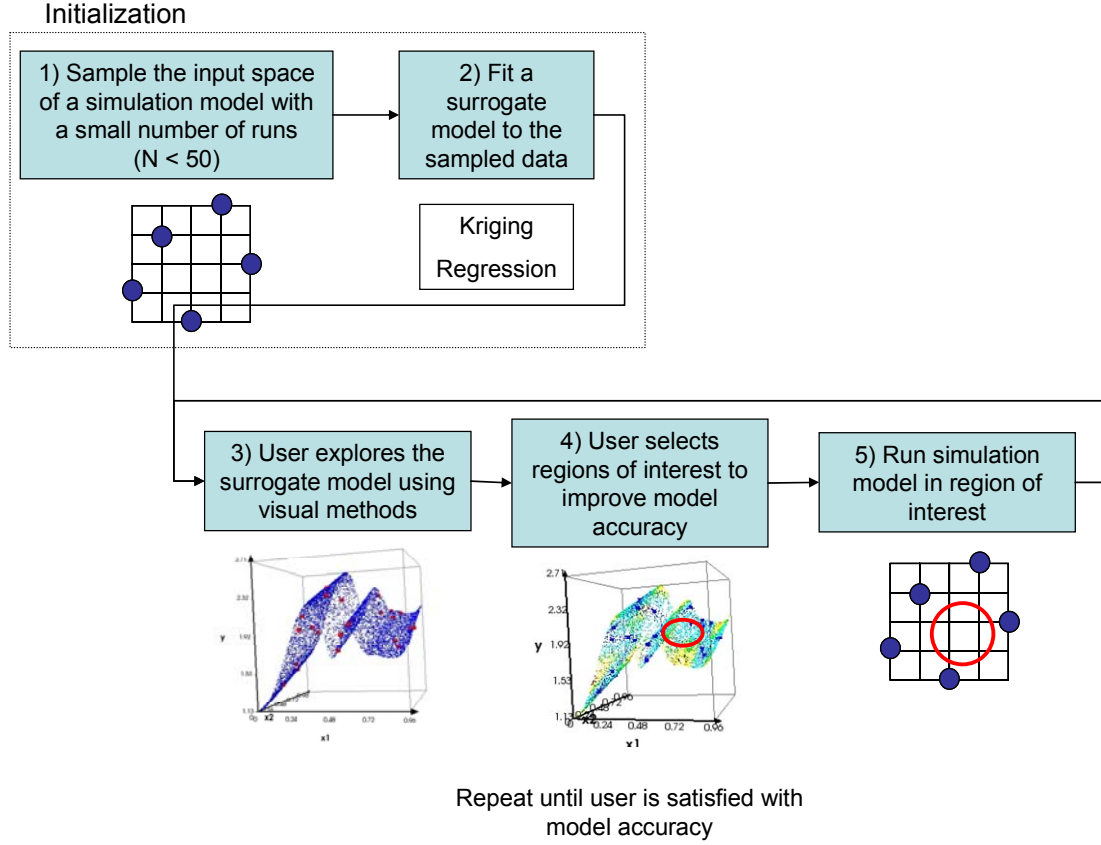


Figure 3. Approach to update surrogate models

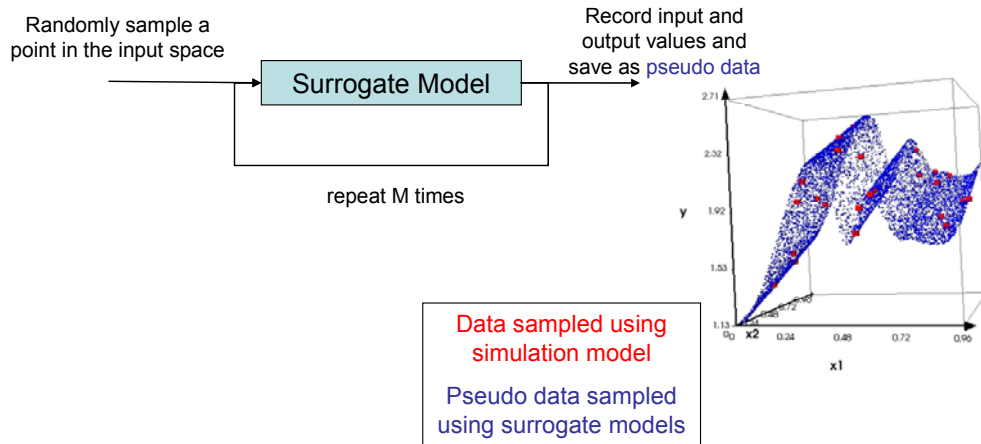


Figure 4. Pseudo data generated using surrogate models

B. Demonstration Example

The process of refining a surrogate model is demonstrated by using the five steps from above with a simple example with 2 inputs (x_1 , x_2) and 1 output often called the “Mystery” function.¹⁵ Both input values are continuous [0,5], and the output variable has the following equation:

$$y = 2 + 0.01(x_2 - x_1^2)^2 + (1 - x_1) + 2(2 - x_2)^2 + 7 \sin(0.5x_1) \sin(0.7x_1x_2) \quad (10)$$

Step 1 The process starts by evaluating an initial 25 points selected using a Latin Hypercube to sample the design space as shown in Figure 5.

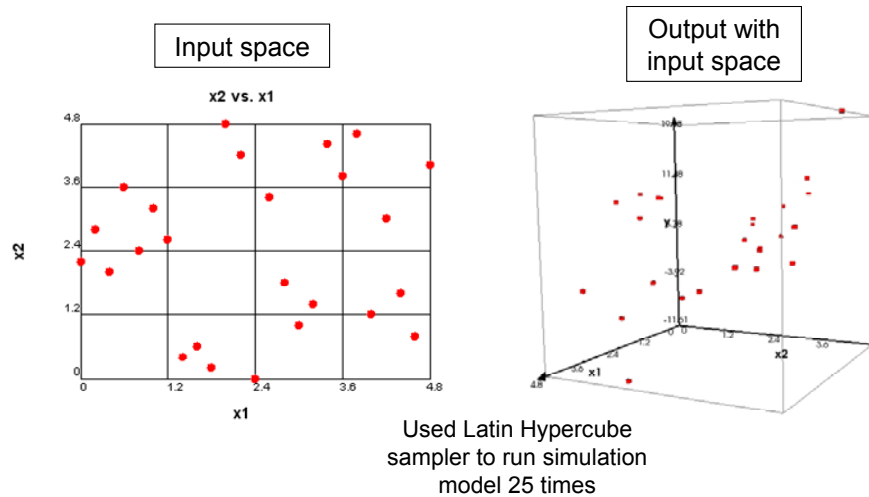


Figure 5. 2D scatter plot of input space, and 3D scatter plot of output variable with input variables

Step 2 A kriging model is created using Eqs. 1-9 based on these initial 25 sample points, where the model form and parameter estimation method is selected by the user as shown in Figure 6.

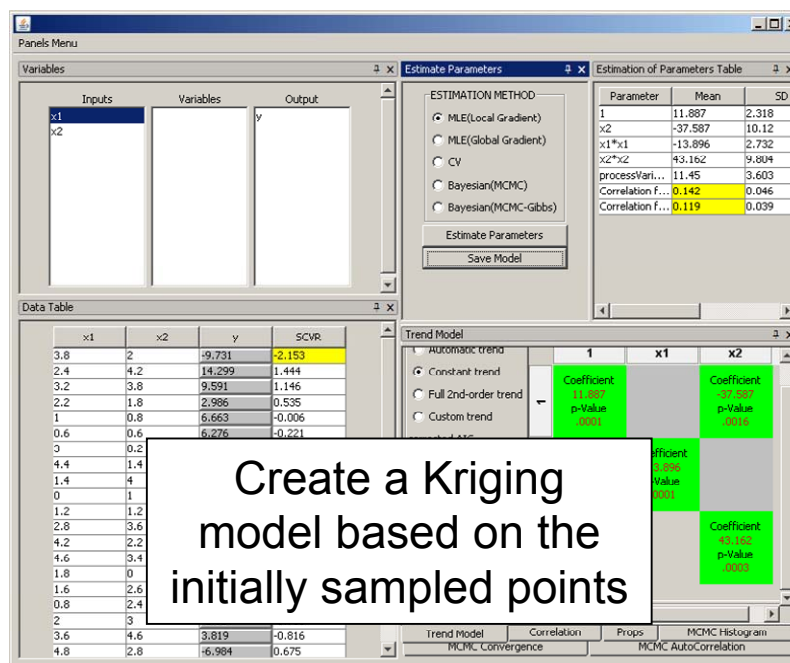


Figure 6. GUI that allows a user to set Kriging terms and correlation methods

Step 3 A Monte Carlo simulation is performed by running the kriging model 10,000 times to generate pseudo data. The results are displayed in a 3D scatter plot shown in Figure 7. All of the pseudo points are displayed in blue while the actual observations used to create the surrogate are shown in red. The use of pseudo points to display the response surface as a translucent cloud allows the user to see through and observe the behavior in the trade space.

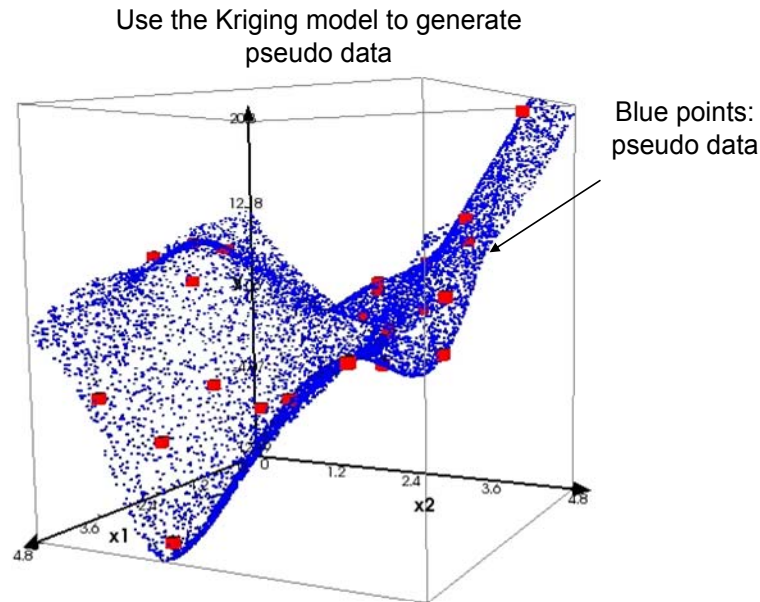


Figure 7. Pseudo data is generated by the Kriging model

- Step 4** The areas of interest are identified and a point to update the kriging model is selected. The standard deviation (square root of the mean squared error) of the kriging model's estimate is assigned a color within the 3D scatter plot. As illustrated in Figure 8, regions of the response surface shaded in red have the highest amount of uncertainty, where regions shaded in blue have a low amount of uncertainty.
- Step 5** The kriging surrogate model is updated with a new observation of the original model, executed at the selected pseudo point. The rest of the plots in Figure 8 demonstrate the use of this analysis tool to repeat steps 3-5 to update the surrogate model. The region in the lower left-hand side of the plot is chosen as the area of interest and highest uncertainty values within this region are continually selected to improve the kriging model in the region of interest.

This example demonstrates the process of a user selecting areas within the region of interest that have high uncertainty; these new points are sent to the high fidelity simulation model, which then appends this new design to the kriging model. The kriging model is refined with the new point, and the process is repeated until the region of interest has an acceptable level of uncertainty.

The response of the original function, the “real surface”, is displayed in addition to the surrogate response surface that has been updated with the additional point in the region of interest in Figure 9. The overall benefits of this approach can be observed in the low amount of discrepancies between the surrogate and the real surfaces in the regions of interest. The response surface has higher errors in other regions, but accuracy in these regions is not important.

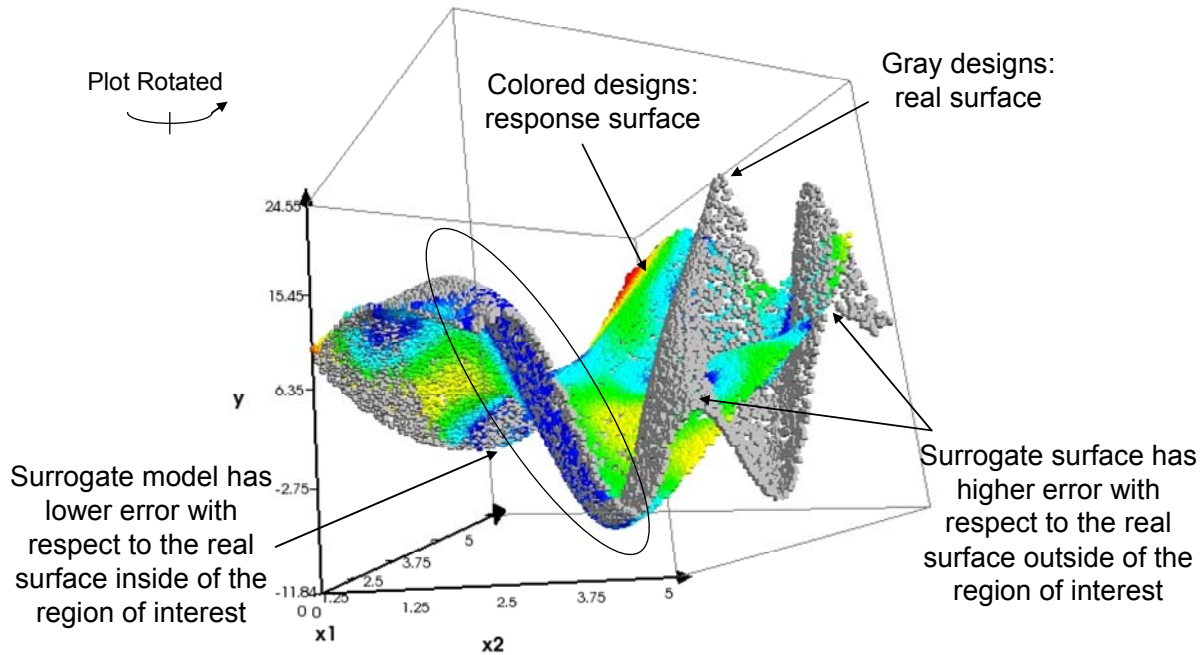


Figure 9. Comparison of the surrogate model with the real data

IV. Fuel Tank Model Example

The fuel tank design example was originally developed by Dr. Jaroslaw Sobieski, formerly of NASA Langley Research Center in Hampton, VA, to illustrate how changes in a problem's objective function influence the resulting optimal design.¹⁶ The overall objective is to improve NASA's Return on Investment (ROI) for the Space Shuttle by resizing its external fuel tank. The external fuel tank is divided into three hollow geometric segments: (1) a cylinder (length L , radius R), (2) a hemispherical end cap (radius R), and (3) a conical nose (height h , radius R), as shown in Figure 10. Space Shuttle external fuel tank¹⁶Figure 10. These segments have thicknesses t_1 , t_2 , and t_3 , respectively. Each segment is assumed to be a monocoque shell constructed from aluminum and welded together from four separate pieces of material, resulting in a total of fourteen welded seams. Surface areas and volumes are determined using geometric relations, and first principles and rules of thumb are used to calculate stresses, vibration modes, aerodynamic drag, and cost using the analyses described by Schuman, et al.¹⁶

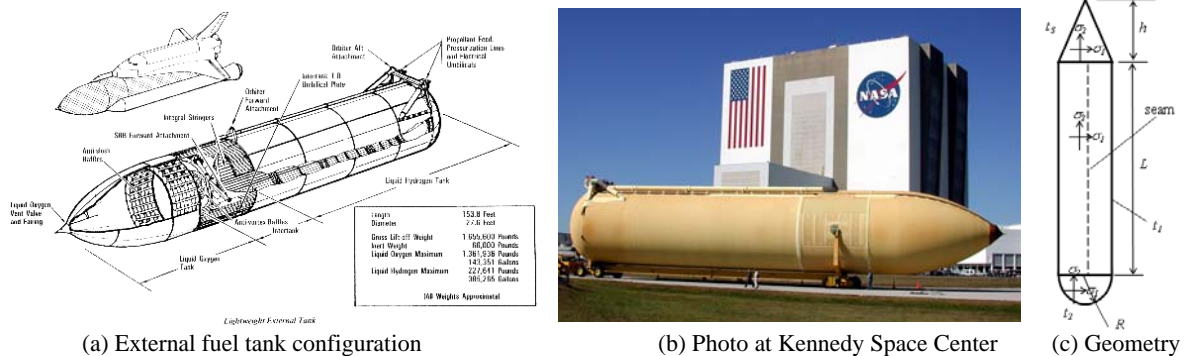


Figure 10. Space Shuttle external fuel tank¹⁶

The optimization problem is formulated based on the original model as follows:

Maximize: ROI (10)
Subject to: Volume constraint:

$$2826 \leq V_t \leq 3026 \Rightarrow |V_t - 100| - 2926 \leq 0$$

Stress and vibration constraints

$$\sigma_{e,i} \leq 4 \cdot 10^8 \Rightarrow \sigma_{e,i} - 4 \cdot 10^8 \leq 0$$

$$0.8 \leq \zeta \Rightarrow 0.8 - \zeta \leq 0$$

Design variables bounds:

$$0.01 \leq L_n \leq 5.0$$

$$0.25 \leq t_{2n} \leq 2.0$$

$$0.50 \leq R_n \leq 2.0$$

$$0.25 \leq t_{3n} \leq 2.0$$

$$0.25 \leq t_{1n} \leq 2.0$$

$$0.10 \leq h/R_n \leq 5.0$$

The objective is to maximize ROI subject to the constraints on the tank volume and stresses and bounds on the design variables. The restriction on tank volume is an equality constraint ($\sim 3000 \text{ m}^3 \pm 100 \text{ m}^3$), which has been found difficult to meet when using ATSV. The tank volume is dependent upon three parameters (L , R , h/R). It has been reformulated so that the designer can vary any two parameters while the third is dependent upon these two by enforcing a volume constraint (i.e., specify values for R and h/R and compute L to satisfy the volume constraint). Finally, inequality constraints are placed on the maximum allowable component stress and on the first bending moment of the tank. The equivalent stress experienced by each component cannot exceed the maximum allowable stress of the material is used. Also, the first bending moment of the tank must be kept away from the vibrational frequencies experienced during launch to avoid any potential failures.

The first step in the approach is to randomly sample the feasible trade space by varying the length, radius, and and three thicknesses of the external fuel tank. The resulting feasible designs are displayed in Figure 11.

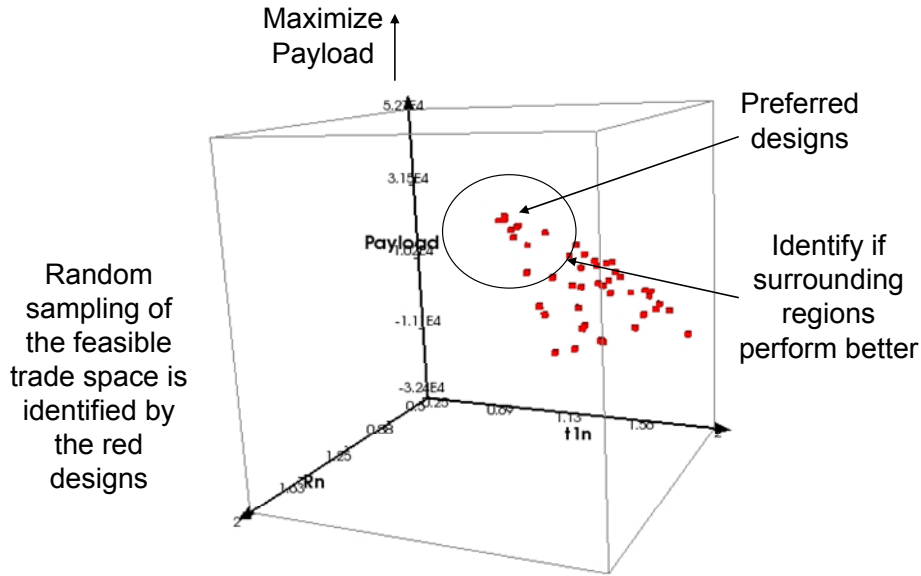


Figure 11. Initial feasible trade space

A kriging model for payload is created based on the initial feasible set of designs. In Figure 12, the original feasible designs are displayed as large blue cubes, and the kriging model is displayed using small cubes, where color identifies the model uncertainty. The resulting kriging model identifies a region of interest, where the payload has higher values. To identify if any neighboring regions within the surrogate model perform better with respect to payload, additional high fidelity design samples are calculated, as shown in Figure 13.

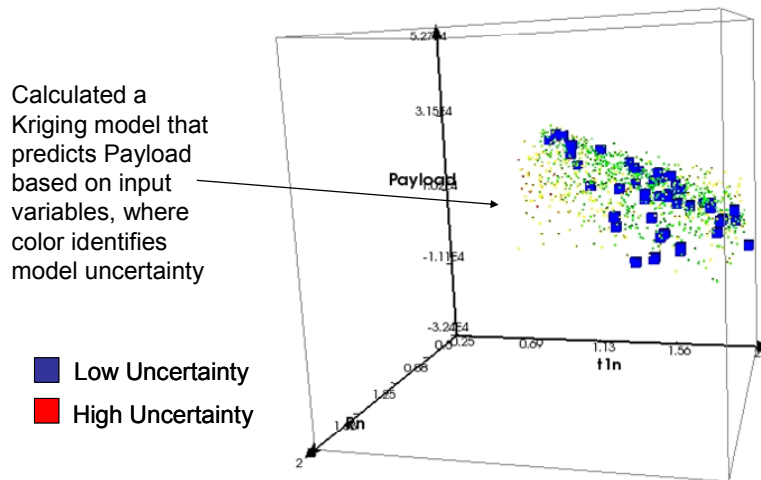


Figure 12. Kriging model that approximates payload based on input values

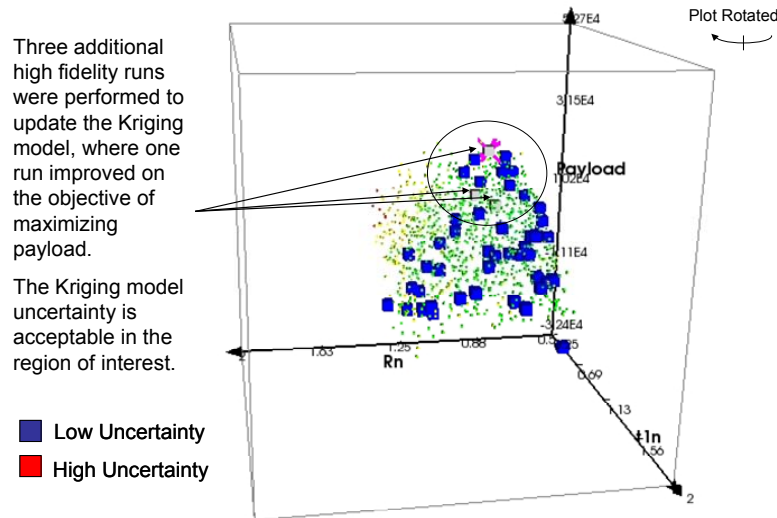


Figure 13. Additional high fidelity designs are sampled in the region of interest

A comparison of the using the kriging model approximation to select a desired design was made to the previous method of using the high fidelity model to generate the design space. The comparison starts with the selection of the most preferred design, which is a high fidelity run, identified by a purple icon in Figure 13. This icon is saved within the plot, and an evolutionary optimization strategy is applied to the high fidelity fuel tank model, where the objective of the problem is to maximize Payload. The optimizer calculated 500 designs, and the results of this optimization run are displayed Figure 14, where all of the designs in blue represent the optimization runs. The best value calculated by the optimizer performed slightly better than the refined surrogate model. This demonstrates the key advantage and disadvantage of using visual tools to refine kriging models, where a very good design can be calculated with a lower number of high fidelity runs with a penalty in objective value performance.

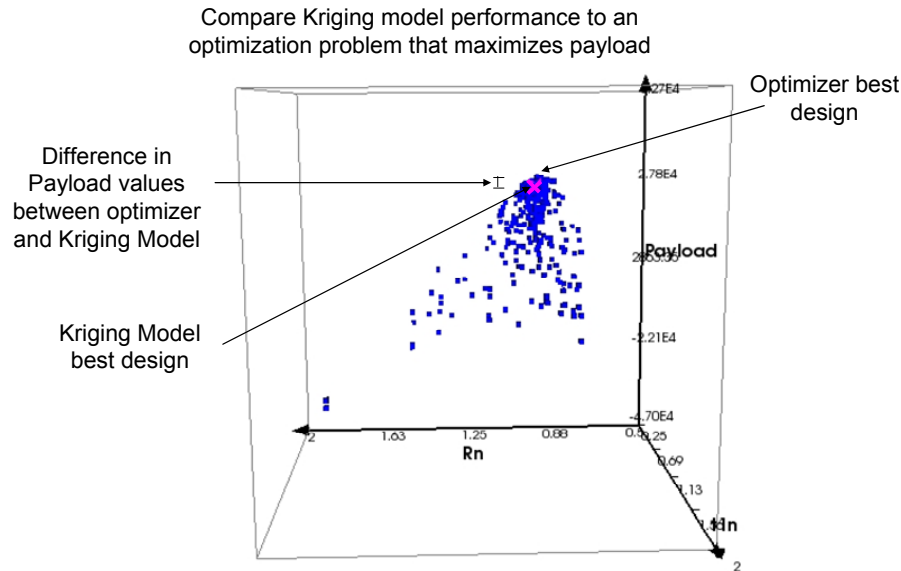


Figure 14. Visualization of kriging model performance and optimum design

V. Closing Remarks and Future Work

In closing, an approach that supports a human-in-the-loop process, where users can refine surrogate models using multidimensional data visualization methods, is proposed and demonstrated. This approach allows users to visualize both high fidelity simulation model data and surrogate model data within multidimensional data visualization plots. This interactive capability provides a user with more intuitive tools to refine the surrogate models in locations of the trade space that are of interest, thereby minimizing the number of high cost simulation analyses that may need to be performed. The interactive process also gives the user a better understanding of the trade space's variability and the uncertainty that exists in regions between the observations of the high fidelity models. It also provides an approach to allow the user to select new locations to execute the high fidelity models to improve the current representation of the design space by focusing on regions of interest and by reducing the uncertainty within these regions of interest.

Future work can focus on supporting this design trade space improvement process on more complex multidisciplinary systems. The proposed approach has been prototyped on example test problems, but the overall method needs to be refined to support a larger-scale problems with more inputs. Currently, kriging correlation coefficients are optimized after each run, which could become time intensive for large-scale problems. More efficient methods to update existing kriging models with new runs can be included within the proposed approach.¹⁷

Acknowledgments

This work is supported in part by the National Foundation under Grant No. CMMI-0620948 and by the Office of Naval Research under contract number N00014-10-G-0259. Any opinions, findings, and conclusions or recommendations presented in this paper are those of the authors and do not necessarily reflect the views of the National Science Foundation or the Office of Naval Research.

References

- ¹Balling, R., "Design by Shopping: A New Paradigm?" *Proceedings of the Third World Congress of Structural and Multidisciplinary Optimization (WCSMO-3)*, Buffalo, NY, University at Buffalo, 1999, pp. 295-297.
- ²Hwang, C.-L. and Masud, A. S., *Multiple Objective Decision Making - Methods and Applications*, New York, Springer-Verlag, 1979.
- ³Simpson, T. W., Spencer, D. B. and Yukish, M. A., "Visual Steering Commands and Test Problems to Support Research in Trade Space Exploration", *12th AIAA/ISSMO Multidisciplinary Analysis and Optimization Conference*, Victoria, British Columbia, Canada, AIAA, 2008, AIAA-2008-6085.
- ⁴Stump, G., Yukish, M. and Simpson, T. W., "The ARL Trade Space Visualizer: An Engineering Decision-Making Tool", *10th AIAA/ISSMO Multidisciplinary Analysis and Optimization Conference*, Albany, NY, AIAA, 2004, AIAA-2004-4568.
- ⁵Wang, G. G. and Shan, S., "Review of Metamodeling Techniques in Support of Engineering Design Optimization," *ASME Journal of Mechanical Design*, Vol. 129, No. 4, 2007, pp. 370-380.

- ⁶Lin, Y., Luo, D., Bailey, T., Khire, R., Wang, J. and Simpson, T. W., "Model Validation and Error Modeling to Support Sequential Sampling", *ASME Design Engineering Technical Conferences - Design Automation Conference*, New York, NY, ASME, 2008, DETC2008/DAC-49336.
- ⁷Martin, J. D. and Simpson, T. W., "On the Use of Kriging Models to Approximate Deterministic Computer Models," *AIAA Journal*, Vol. 43, No. 4, 2005, pp. 853-863.
- ⁸Simpson, T. W., Peplinski, J., Koch, P. N. and Allen, J. K., "Metamodels for Computer-Based Engineering Design: Survey and Recommendations," *Engineering with Computers*, Vol. 17, No. 2, 2001, pp. 129-150.
- ⁹Martin, J. D., "Computational Improvements to Estimating Kriging Metamodel Parameters," *ASME Journal of Mechanical Design*, Vol. 131, No. 8, 2009, pp. 084501.
- ¹⁰Stump, G., Yukish, M., Simpson, T. W., Harris, E. N. and O'Hara, J. J., "Trade Space Exploration of Satellite Datasets Using a Design by Shopping Paradigm", *IEEE Aerospace Conference*, Big Sky, MT, IEEE, 2004, IEEE-1039-04.
- ¹¹Stump, G., Lego, S., Yukish, M., Simpson, T. W. and Donndelinger, J. A., "Visual Steering Commands for Trade Space Exploration: User-Guided Sampling with Example," *ASME Journal of Computing and Information Science in Engineering*, Vol. 9, No. 4, 2009, pp. 044501 (10 pgs).
- ¹²Simpson, T. W., Mauery, T. M., Korte, J. J. and Mistree, F., "Kriging Metamodels for Global Approximation in Simulation-Based Multidisciplinary Design Optimization," *AIAA Journal*, Vol. 39, No. 12, 2001, pp. 2233-2241.
- ¹³McKay, M. D., Beckman, R. J. and Conover, W. J., "A Comparison of Three Methods for Selecting Values of Input Variables in the Analysis of Output from a Computer Code," *Technometrics*, Vol. 21, No. 2, 1979, pp. 239-245.
- ¹⁴Martin, J. D. and Simpson, T. W., "A Methodology to Manage System-Level Uncertainty during Conceptual Design," *ASME Journal of Mechanical Design*, Vol. 128, No. 4, 2006, pp. 959-968.
- ¹⁵Sasena, M. J., 2002, Flexibility and Efficiency Enhancements for Constrained Global Design Optimization with Kriging Approximations, Mechanical Engineering. Ann Arbor, MI, Univeristy of Michigan. Ph. D.
- ¹⁶Schuman, T., de Weck, O. L. and Sobieski, J., "Integrated System-Level Optimization for Concurrent Engineering with Parametric Subsystem Modeling", *1st Multidisciplinary Design Optimization Specialist Conference*, Austin, TX, AIAA, 2005, AIAA-2005-2199.
- ¹⁷Gano, S. E., Renaud, J. E., Martin, J. D. and Simpson, T. W., "Update Strategies for Kriging Models for Using in Variable Fidelity Optimization," *Structural and Multidisciplinary Optimization*, Vol. 32, No. 4, 2006, pp. 287-298.